

High-Order Entropy-Conservative Schemes and Kinetic Relations for van der Waals Fluids

C. Chalons* and P. G. LeFloch†

*O.N.E.R.A., B.P. 72, 29 Avenue de la Division Leclerc, 92322 Châtillon Cedex, France; and †Centre de Mathématiques Appliquées & Centre National de la Recherche Scientifique, U.M.R. 7641, Ecole Polytechnique, 91128 Palaiseau Cedex, France
E-mail: chalons@onera.fr, lefloch@cmap.polytechnique.fr

Received July 20, 2000; revised November 27, 2000

We consider the mixed (hyperbolic–elliptic) system of two conservation laws modeling the dynamics of van der Waals fluids. Viscosity and capillarity effects are taken into account. We introduce a new class of semidiscrete *high-order schemes* which are *entropy conservative* (in the sense of Tadmor) when the viscosity is neglected and, otherwise, dissipate the associated mathematical entropy. Our numerical schemes generalize the works by E. Tadmor (1987, *Math. Comput.* **49**, 91) and P. G. LeFloch and C. Rohde (2000, *SIAM J. Numer. Anal.* **37**, 2023) who proposed second-order and third-order entropy-conservative schemes, respectively.

Following B. T. Hayes and P. G. LeFloch (1998, *SIAM J. Numer. Anal.* **35**, 2169), we demonstrate numerically that balanced viscosity and capillarity terms in van der Waals fluids may generate *nonclassical shock waves* or *subsonic propagating phase transitions*. Such waves are *undercompressive* and do not satisfy standard entropy criteria. They must be characterized by a *kinetic function*, which we determine numerically in this paper from vanishing viscosity and capillarity. The kinetic relation is an efficient tool to discuss the interplay among the viscosity, capillarity, and discretization parameters in van der Waals fluids. © 2001 Academic Press

Key Words: hyperbolic; conservation law; entropy inequality; viscosity; capillarity; van der Waals; kinetic relation; difference scheme; high-order accurate; entropy conservative.

1. INTRODUCTION

The dynamics of compressible fluids undergoing liquid–solid or vapor–liquid phase transformations can be modeled by the standard balance laws (mass, momentum) supplemented with a nonconvex equation of state, such as the one introduced by van der Waals. Restricted attention to a model of two conservation laws (the temperature being, formally, kept

constant), one knows that, above some (critical) temperature this model is hyperbolic but not globally genuinely nonlinear (the pressure is a decreasing but not a globally convex function of the specific volume); however, below the critical temperature, the model is a mixed (hyperbolic–elliptic) system of conservation laws (the pressure is decreasing except on some bounded interval). Solutions of such systems of nonlinear PDEs are generally discontinuous and exhibit several distinct types of propagating waves:

- (1) compressive shock waves satisfying the standard Lax or Liu entropy criteria;
- (2) rarefaction waves, which are smooth and self-similar solutions;
- (3) supersonic phase boundaries, which propagate faster than the characteristic speed; and
- (4) In the mixed type case, stationary phase boundaries.

Until recently the Riemann problem—for which the initial datum is a single step function—was solved allowing only stationary and supersonic phase boundaries plus standard classical waves [12, 23]. Recently, after the works by James [17], Truskinovsky [32, 33], Slemrod [26], Abeyaratne and Knowles [1, 2], LeFloch [19–21], Shearer *et al.* [16, 24], and Hayes and LeFloch [13–15], it became clear that nonstationary, subsonic phase interfaces (in the hyperbolic–elliptic regime) and nonclassical shock waves (in the hyperbolic, but not genuinely nonlinear regime) should be included when solving the Riemann problem. Indeed, such waves are admissible in the sense that they do arise in viscosity–capillarity limits of the system.

Subsonic phase boundaries and nonclassical shocks have a special flavor: they are not uniquely characterized by the standard Rankine–Hugoniot relations and their unique selection requires an *additional jump relation* called a *kinetic relation*. Recall that there is indeed no universal selection criterion for propagating phase boundaries. The basic reason is that such waves are *undercompressive*, in the sense that—compared with compressive shocks—fewer characteristics are impinging on the discontinuity.

The numerical approximation of the model under consideration was initiated by Slemrod and followers [3, 5, 18, 25, 29]. Computing kinetic relations to characterize undercompressive waves such as nonclassical shocks and subsonic phase boundaries was first tackled by Hayes and LeFloch [15], who identified the basic issues arising numerically. The present paper is a natural extension of [15].

In Section 2 we discuss the mathematical properties of the system modeling the dynamics of fluids with viscosity and capillarity effects included. Special emphasis is put on the mathematical entropy inequality, here associated with the total energy.

In Section 3 we introduce a new class of semidiscrete, *high-order schemes* which are *entropy conservative* (in the sense of Tadmor) if the viscosity term is neglected and, otherwise, satisfy a *discrete entropy inequality*. Our construction is inspired by Tadmor [30, 31] and LeFloch and Rohde [22] who derived earlier second-order and third-order entropy-conservative schemes, respectively. The main new idea is to treat as an independent variable the derivative of one of the conservative variables, here v_y , where v is the specific volume. An evolution equation for v_y is formulated and discretized in the scheme. An important observation is that an entropy inequality can indeed be derived.

In Sections 4 and 5 we show that our numerical scheme allows us to compute subsonic phase boundaries and nonclassical shock waves. We consider here the Riemann problem investigated theoretically by Slemrod [28] and Fan [7–10]. Following Hayes and LeFloch [14], who studied nonconvex scalar conservation laws and phase transition models from

nonlinear elasticity theory, we determine numerically the kinetic function associated with van der Waals fluids and we discuss the interplay among the viscosity, capillarity, and discretization parameters. Concluding remarks are provided in Section 6.

2. VISCOSITY–CAPILLARITY MODEL OF COMPRESSIBLE FLUIDS

2.1. The Mathematical Formulation

The derivation of the equations is based on a variational formulation. See, for instance, the presentation given in Gavriluk and Gouin [6]. Let $(y, t) \mapsto \chi(y, t)$ be the Lagrangian description of the fluid motion. That is, by definition, the particle which was initially at the position y is located at the point $\chi(y, t)$ at the time t . The particle velocity u and the specific volume v are defined from χ by

$$u = \chi_t, \quad v = \chi_y. \quad (2.1)$$

Prescribing an internal energy function of the form

$$e = e(v, v_y),$$

we postulate that the action

$$J(\chi) = \int_0^T \int_{\Omega} \left(e(v, v_y) - \frac{u^2}{2} \right) dy dt = \int_0^T \int_{\Omega} \left(e(\chi_y, \chi_{yy}) - \frac{\chi_t^2}{2} \right) dy dt \quad (2.2)$$

is minimal among all “admissible” χ . Here, $\Omega \subset \mathbb{R}$ is the (bounded) interval initially occupied by the fluid and $[0, T]$ is a given time interval.

Let $g : \Omega \times [0, T] \rightarrow \mathbb{R}$ be a smooth function with compact support. Replacing in (2.2) χ with $\chi + g$ and keeping the first-order terms in g only, we obtain

$$\begin{aligned} J(\chi + g) &= \int_0^T \int_{\Omega} \left(e(\chi_y + g_y, \chi_{yy} + g_{yy}) - \frac{1}{2}(\chi_t + g_t)^2 \right) dy dt \\ &= J(\chi) + \int_0^T \int_{\Omega} \left(\frac{\partial e}{\partial \chi_y}(\chi_y, \chi_{yy})g_y + \frac{\partial e}{\partial \chi_{yy}}(\chi_y, \chi_{yy})g_{yy} - \chi_t g_t \right) dy dt \\ &\quad + O(|g|^2) \end{aligned}$$

and, after integration by parts,

$$\begin{aligned} J(\chi + g) &= J(\chi) + \int_0^T \int_{\Omega} \left(\left(-\frac{\partial e}{\partial \chi_y}(\chi_y, \chi_{yy}) \right)_y \right. \\ &\quad \left. + \left(\frac{\partial e}{\partial \chi_{yy}}(\chi_y, \chi_{yy}) \right)_{yy} + \chi_{tt} \right) g dy dt + O(|g|^2). \end{aligned}$$

Since the solution χ should minimize the action J and g is arbitrary, this formally yields

$$\chi_{tt} + \left(-\frac{\partial e}{\partial \chi_y}(\chi_y, \chi_{yy}) + \left(\frac{\partial e}{\partial \chi_{yy}}(\chi_y, \chi_{yy}) \right)_y \right)_y = 0. \quad (2.3)$$

Returning to the functions u and v , in view of (2.1) we also have $v_t = \chi_{yt} = u_y$. Introducing the pressure term

$$P(v, v_y, v_{yy}) = -\frac{\partial e}{\partial v}(v, v_y) + \left(\frac{\partial e}{\partial v_y}(v, v_y) \right)_y, \quad (2.4)$$

we deduce from (2.1) and (2.3) that

$$\begin{aligned} v_t - u_y &= 0, \\ u_t + P(v, v_y, v_{yy})_y &= 0. \end{aligned} \quad (2.5)$$

This completes the derivation of the fluid model for the unknowns v and u .

Next, we take into account the viscosity effects. Denoting by $\mu(v)$ the (volume-dependent) viscosity coefficient of the fluid, we replace system (2.5) with

$$\begin{aligned} v_t - u_y &= 0, \\ u_t + P(v, v_y, v_{yy})_y &= (\mu(v)u_y)_y. \end{aligned} \quad (2.6)$$

Finally, defining the total energy by

$$E(v, u, v_y) = e(v, v_y) + \frac{u^2}{2},$$

we find the additional conservation law

$$E(v, u, v_y)_t + (P(v, v_y, v_{yy})u)_y = \left(u_y \frac{\partial e}{\partial v_y}(v, v_y) \right)_y + (\mu(v)uu_y)_y - \mu(v)u_y^2. \quad (2.7)$$

Here the energy plays the role of a mathematical entropy.

It remains to discuss the properties of the internal energy function e . A standard choice in the literature on phase transition dynamics in fluids is to take e to be a quadratic function in v_y . (A linear term should not appear because of the invariance of the energy via the transformation $y \mapsto -y$.) We may assume that, for some positive function $\lambda(v)$, called the *capillarity coefficient*,

$$e(v, v_y) = \epsilon(v) + \lambda(v) \frac{v_y^2}{2}. \quad (2.8)$$

Under this condition, the total pressure P can be decomposed into a pressure term depending only on v and a capillarity term, as follows:

$$P(v, v_y, v_{yy}) = p(v) - \lambda'(v) \frac{v_y^2}{2} + (\lambda(v)v_y)_y, \quad p(v) = -\epsilon'(v). \quad (2.9)$$

Based on (2.9), Eq. (2.6) take the more familiar form

$$\begin{aligned} v_t - u_y &= 0, \\ u_t + p(v)_y &= \left(\lambda'(v) \frac{v_y^2}{2} - (\lambda(v)v_y)_y \right)_y + (\mu(v)u_y)_y. \end{aligned} \quad (2.10)$$

On the other hand, using (2.9), Eq. (2.7) becomes

$$\begin{aligned} & \left(\epsilon(v) + \frac{u^2}{2} + \lambda(v) \frac{v_y^2}{2} \right)_t + (p(v)u)_y \\ &= \left(u \left(\frac{\lambda'(v)}{2} v_y^2 - (\lambda(v)v_y)_y \right) \right)_y + (\mu(v)uu_y)_y + (u_y \lambda(v)v_y)_y - \mu(v)u_y^2. \end{aligned} \quad (2.11)$$

We point out that this model has been often considered in the mathematical literature on phase transition dynamics, under the simplifying assumption that the capillarity $\lambda(v) = \lambda_0$ be a positive constant.

2.2. Hyperbolicity and Decrease of the Mathematical Entropy

It is immediate to check the following property. Consider the linearization of the model (2.4), (2.5) near some constant value v_0 given by

$$\begin{aligned} v_t - u_y &= 0, \\ u_t - \frac{\partial^2 e}{\partial^2 v}(v_0, 0)v_y &= 0, \end{aligned} \quad (2.12)$$

obtained by keeping first-order differential terms only. Then (2.12) is a strictly hyperbolic system of PDEs if and only if the internal energy function satisfies

$$\frac{\partial^2 e}{\partial^2 v}(v_0, 0) > 0. \quad (2.13)$$

Moreover, if (2.13) holds for all v_0 , then the total energy $E(v, u, 0) = e(v, 0) + u^2/2$ is a strictly convex function of the conservative variables (v, u) . For van der Waals fluids, the hyperbolicity condition holds only in some regions. See Section 4.

Given some internal energy function $e = e(v, v_y)$ and some nonlinear viscosity $\mu = \mu(v) > 0$, let us consider the corresponding viscosity–capillarity model (2.6), where the pressure $P(v, v_y)$ is defined by (2.4). Consider any solution $(y, t) \mapsto (v, u)(y, t)$ decaying to some constant solution (v^*, u^*) as $|y| \rightarrow \infty$ (its first-order space derivative also vanishing at infinity) Then we have

$$\frac{d}{dt} \varepsilon(t) \leq 0, \quad (2.14)$$

where

$$\varepsilon(t) := \int_{\mathbb{R}} \left(e(v(y, t), v_y(y, t)) - e(v^*, 0) - \frac{\partial e}{\partial v}(v^*, 0)(v(y, t) - v^*) + \frac{u(y, t)^2}{2} \right) dy.$$

We conclude with some remarks concerning the hyperbolic regime.

For the example (2.8), the condition (2.13) reads $\epsilon''(v) > 0$. Let us assume the uniform bound

$$0 < \epsilon_0 \leq \epsilon''(v) \leq \epsilon_1 \quad \text{for all } v > 0.$$

We have here

$$e(v, v_y) - e(v^*, 0) - \frac{\partial e}{\partial v}(v^*, 0)(v - v^*) = \epsilon(v) - \epsilon(v^*) - \epsilon'(v^*)(v - v^*) + \lambda(v) \frac{v_y^2}{2}.$$

Therefore, assuming also some bounds

$$\lambda_0 \leq \lambda(v) \leq \lambda_1 \quad \text{for all } v > 0,$$

(2.14) yields the following a priori bound (for all $t \geq 0$):

$$\begin{aligned} & \int_{\mathbb{R}} (\epsilon_0 |v(y, t) - v^*|^2 + |u(y, t) - u^*|^2 + \lambda_0 v_y^2) dy \\ & \leq \int_{\mathbb{R}} (\epsilon_1 |v(y, 0) - v^*|^2 + |u(y, 0) - u^*|^2 + \lambda_1 v_y^2) dy. \end{aligned}$$

More generally, if the energy function satisfies inequalities of the form

$$\begin{aligned} \frac{\epsilon_0}{2} |v - v^*|^2 + \frac{\beta_0}{2} |v_y|^2 & \leq e(v, v_y) - e(v^*, 0) - \frac{\partial e}{\partial v}(v^*, 0)(v - v^*) \\ & \leq \frac{\epsilon_1}{2} |v - v^*|^2 + \frac{\beta_1}{2} |v_y|^2 \end{aligned}$$

for all v and v_y under consideration, then the following a priori estimate holds for all times t :

$$\begin{aligned} & \int_{\mathbb{R}} (\epsilon_0 |v(y, t) - v^*|^2 + |u(y, t) - u^*|^2 + \beta_0 |v_y(y, t)|^2) dy \\ & \leq \int_{\mathbb{R}} (\epsilon_1 |v(y, 0) - v^*|^2 + |u(y, 0) - u^*|^2 + \beta_1 |v_y(y, 0)|^2) dy. \end{aligned}$$

3. A CLASS OF ENTROPY CONSISTENT SCHEMES

In this section, we focus on the numerical discretization of the model described in Section 2. Our objective is to derive a class of high-order, conservative, finite-difference schemes that, additionally, are conservative for the associated mathematical entropy E when the viscosity effects are neglected and satisfy the discrete entropy inequality (2.14).

Our main concern is to design a scheme able to capture the zero viscosity–capillarity limits. Therefore, following Hayes and LeFloch [13], we are going to scale out all of the equation using the discretization parameter denoted by h ; see Eqs. (3.1), (3.2), and (3.4) below. Then the basic requirement is that the equivalent equation associated with the scheme should coincide up to some high-order term $O(h^3)$, at least, with these reference (continuous) equations.

Comparing rigorously the limiting solutions generated by the schemes and the limiting solutions generated by the zero viscosity–capillarity limits is the main contribution in [13] and this is the strategy pursued in the present work as well. We refer to the discussion in the following sections.

3.1. Discretization of the Flux and Capillarity Terms

Consider first the model (2.4), (2.5), neglecting the viscosity. Introducing the new variables

$$w = h v_y, \quad z = h u_y,$$

we can consider w as an independent variable. We summarize the set of equations under consideration as follows:

$$\begin{aligned} v_t - u_y &= 0, \\ u_t + P_y &= 0, \\ w_t - z_y &= 0. \end{aligned} \tag{3.1}$$

Recall that P is given by

$$P = -\frac{\partial e}{\partial v}(v, w) + h \left(\frac{\partial e}{\partial v_y}(v, w) \right)_y. \tag{3.2}$$

Denote by $h > 0$ the space step of the discretization and, for all integer j , define the mesh point by $x_j = j h$. We denote by $v_j = v_j(t)$, $u_j = u_j(t)$, and $w_j = w_j(t)$ the discrete approximations at the points x_j (with prescribed initial conditions). Calling $u_{j+1/2}$, $P_{j+1/2}$, and $z_{j+1/2}$ some numerical flux terms still to be defined, we are interested in difference schemes in the following conservative form:

$$\begin{aligned} h \frac{d}{dt} v_j - (u_{j+1/2} - u_{j-1/2}) &= 0, \\ h \frac{d}{dt} u_j + P_{j+1/2} - P_{j-1/2} &= 0, \\ h \frac{d}{dt} w_j - (z_{j+1/2} - z_{j-1/2}) &= 0. \end{aligned} \tag{3.3}$$

We aim at defining the discrete fluxes $u_{j+1/2}$, $P_{j+1/2}$, and $z_{j+1/2}$ in such a way that the scheme (3.3) is also entropy conservative in the sense of [31]. That is, we seek for a discrete version of the energy equation

$$\begin{aligned} \partial_t E + \partial_y F &= 0, \\ E = e(v, w) + \frac{u^2}{2}, \quad F = P(v, w, h w_y) u - h u_y \frac{\partial e}{\partial v_y}(v, w). \end{aligned} \tag{3.4}$$

With this in mind, we choose

$$\begin{aligned} u_{j+1/2} &= \sum_{k=-K}^{K+1} \alpha_k u_{j+k}, \\ z_{j+1/2} &= \sum_{l=-L}^L \beta_l (u_{j+1+l} - u_{j+l}), \end{aligned} \tag{3.5}$$

in which the terms u_{j+k} , for instance, are directly given by the second equation in (3.3). A basic consistency argument forces us to impose

$$\sum_{k=-K}^{K+1} \alpha_k = \sum_{l=-L}^L \beta_l = 1. \quad (3.6)$$

It remains to specify the expression for the pressure $P_{j+1/2}$. This is done by requiring the condition

$$\frac{d}{dt} \sum_{j=-\infty}^{+\infty} E_j = 0, \quad E_j = e(v_j, w_j) + \frac{u_j^2}{2}. \quad (3.7)$$

Differentiating the above expression for the energy E_j , we easily obtain

$$h \frac{d}{dt} E_j = h \frac{\partial e}{\partial v}(v_j, w_j) \frac{d}{dt} v_j + h \frac{\partial e}{\partial v_y}(v_j, w_j) \frac{d}{dt} w_j + h u_j \frac{d}{dt} u_j.$$

In view of (3.3) we have

$$\begin{aligned} h \frac{d}{dt} E_j &= \frac{\partial e}{\partial v}(v_j, w_j) (u_{j+1/2} - u_{j-1/2}) - u_j (P_{j+1/2} - P_{j-1/2}) \\ &\quad + \frac{\partial e}{\partial v_u}(v_j, w_j) (z_{j+1/2} - z_{j-1/2}). \end{aligned} \quad (3.8)$$

Using (3.5) and after integration by parts, for instance writing

$$- \sum_{j=-\infty}^{+\infty} u_j (P_{j+1/2} - P_{j-1/2}) = \sum_{j=-\infty}^{+\infty} P_{j+1/2} (u_{j+1} - u_j),$$

we arrive at

$$h \frac{d}{dt} \sum_{j=-\infty}^{+\infty} E_j = \sum_{j=-\infty}^{+\infty} (P_{j+1/2} + Q_{j+1/2} + R_{j+1/2}) (u_{j+1} - u_j)$$

with

$$\begin{aligned} Q_{j+1/2} &= \sum_{k=-K}^{K+1} \alpha_k \frac{\partial e}{\partial v}(v_{j+1-k}, w_{j+1-k}), \\ R_{j+1/2} &= \sum_{l=-L}^{L+1} \beta_l \left(-\frac{\partial e}{\partial v_y}(v_{j+1-l}, w_{j+1-l}) + \frac{\partial e}{\partial v_y}(v_{j-l}, w_{j-l}) \right). \end{aligned}$$

One sufficient condition for (3.7) to hold is to choose $P_{j+1/2}$ according to

$$P_{j+1/2} = -Q_{j+1/2} - R_{j+1/2}.$$

Using the change of variables $k' = 1 - k$ and $l' = -l$, one checks easily that the above definition is equivalent to setting

$$P_{j+1/2} = - \sum_{k=-K}^{K+1} \alpha_k \frac{\partial e}{\partial v}(v_{j+k}, w_{j+k}) + \sum_{l=-L}^L \beta_l \left(\frac{\partial e}{\partial v_y}(v_{j+l+1}, w_{j+l+1}) - \frac{\partial e}{\partial v_y}(v_{j+1}, w_{j+1}) \right). \quad (3.9)$$

This completes the derivation of the scheme for (2.4), (2.5).

3.2. Local Entropy Inequalities

Next we determine some mathematical entropy fluxes for each cell. Replacing $u_{j+1/2}$, $P_{j+1/2}$, and $z_{j+1/2}$ in (3.10) by their definitions, we obtain

$$h \frac{d}{dt} E_j = \sum_{k=-K}^{K+1} \alpha_k (A_{j,k}^{(1)} - A_{j,k}^{(2)}) + \sum_{l=-L}^L \beta_l (B_{j,l}^{(1)} - 2B_{j,l}^{(2)} + B_{j,l}^{(3)}) \quad (3.10)$$

with

$$\begin{aligned} A_{j,k}^{(1)} &= u_{j+k} \frac{\partial e}{\partial v}(v_j, w_j) - u_j \frac{\partial e}{\partial v}(v_{j-k}, w_{j-k}), \\ A_{j,k}^{(2)} &= u_{j+k-1} \frac{\partial e}{\partial v}(v_j, w_j) - u_j \frac{\partial e}{\partial v}(v_{j+1-k}, w_{j+1-k}), \\ B_{j,l}^{(1)} &= u_{j+l-1} \frac{\partial e}{\partial v_y}(v_j, w_j) - u_j \frac{\partial e}{\partial v_y}(v_{j+1-l}, w_{j+1-l}), \\ B_{j,l}^{(2)} &= u_{j+l} \frac{\partial e}{\partial v_y}(v_j, w_j) - u_j \frac{\partial e}{\partial v_y}(v_{j-l}, w_{j-l}), \\ B_{j,l}^{(3)} &= u_{j+l+1} \frac{\partial e}{\partial v_y}(v_j, w_j) - u_j \frac{\partial e}{\partial v_y}(v_{j-1-l}, w_{j-1-l}). \end{aligned}$$

Finally, using decompositions of the type

$$a_{j+k} - a_j = (a_{j+k} + a_{j+k-1} + \cdots + a_{j+1}) - (a_{j+k-1} + a_{j+k-2} + \cdots + a_j),$$

we see that each of the terms above admits a conservative form. This allows us to determine easily a discrete entropy flux $F_{j+1/2}$. We conclude that there exist numerical fluxes $F_{j+1/2}$ (formally consistent with the continuous flux F) such that the following discrete conservation law holds:

$$h \frac{d}{dt} \left(e(v_j, w_j) + \frac{u_j^2}{2} \right) + F_{j+1/2} - F_{j-1/2} = 0. \quad (3.11)$$

In conclusion, the formulas (3.3), (3.5), and (3.9) define a scheme for the unknowns v_j and u_j , which is conservative for all of the equations in (3.3), including the discrete energy

$$E_j = e(v_j, w_j) + u_j^2/2. \quad (3.12)$$

In particular, we have the important stability property

$$\frac{d}{dt} \sum_{j=-\infty}^{\infty} \left(e(v_j, w_j) + \frac{u_j^2}{2} \right) = 0. \quad (3.13)$$

3.3. Discretization of the Viscosity Terms

To complete the description of the numerical scheme, we now take into account the viscosity terms, covering the general case of a nonlinear viscosity coefficient $\mu(v)$. It is sufficient to present the construction in the case of the system where the flux and capillarity terms have been formally neglected, that is,

$$\begin{aligned} v_t &= 0, \\ u_t &= h(\mu(v)u_y)_y, \\ w_t &= 0. \end{aligned} \quad (3.14)$$

Consider the numerical discretization schemes

$$\begin{aligned} h \frac{d}{dt} v_j &= 0, \\ h \frac{d}{dt} u_j &= \mu_{j+1/2} q_{j+1/2} - \mu_{j-1/2} q_{j-1/2}, \\ h \frac{d}{dt} w_j &= 0, \end{aligned} \quad (3.15)$$

with

$$q_{j+1/2} = \sum_{l=-L}^L \beta_l (u_{j+l+1} - u_{j+l}). \quad (3.16)$$

Here the numerical values $\mu_{j+1/2}$ are approximations of sufficiently high order of the nonlinear viscosity $\mu(v)$.

Differentiating the energy E_j defined in (3.12) with respect to t and using (3.15), we obtain

$$h \frac{d}{dt} E_j = u_j (\mu_{j+1/2} q_{j+1/2} - \mu_{j-1/2} q_{j-1/2}).$$

Summing over j and integrating by parts, we obtain

$$\begin{aligned} \sum_{j=-\infty}^{+\infty} \frac{d}{dt} E_j &= - \sum_{j=-\infty}^{+\infty} \mu_{j+1/2} q_{j+1/2} (u_{j+1} - u_j) \\ &= - \sum_{j=-\infty}^{+\infty} \sum_{l=-L}^L \mu_{j+1/2} \beta_l (u_{j+l+1} - u_{j+l}) (u_{j+1} - u_j). \end{aligned}$$

Setting

$$m_{j+l} = u_{j+l+1} - u_{j+l},$$

it follows that

$$\begin{aligned} \sum_{j=-\infty}^{+\infty} \frac{d}{dt} E_j &= - \sum_{j=-\infty}^{+\infty} \sum_{l=-L}^L \mu_{j+1/2} \beta_l m_{j+l} m_j \\ &= - \sum_{j=-\infty}^{+\infty} \sum_{k=j-L}^{j+L} \mu_{j+1/2} \beta_{k-j} m_k m_j. \end{aligned} \tag{3.17}$$

Assume from now on that the coefficients β_l (first introduced in (3.5) and then used again in (3.16)) are chosen such that the (infinite) quadratic form

$$\sum_{j=-\infty}^{+\infty} \sum_{k=j-L}^{j+L} \mu_{j+1/2} \beta_{k-j} m_k m_j \geq 0 \tag{3.18}$$

is nonnegative for all w_k under consideration. Then from (3.17) we deduce that

$$\sum_{j=-\infty}^{+\infty} \frac{d}{dt} E_j \leq 0, \quad E_j = e(v_j, w_j) + \frac{u_j^2}{2}. \tag{3.19}$$

This property is to be compared with the equality found in (3.13) for the flux and capillarity terms.

3.4. Order of Accuracy

The parameters α_k and β_l in (3.5) and (3.16) must be chosen so that (3.6) and (3.19) hold true. We also require that the order of accuracy be sufficiently high so that the equivalent equation associated with the scheme coincides with the original system except for terms of $O(h^3)$.

For fixed values K and L in (3.5) and (3.16), it is always possible to find some coefficients $\alpha_k, k = -K, \dots, K + 1$, and $\beta_l, l = -L, \dots, L$, to guarantee:

$$u_{j+1/2} - u_{j-1/2} = \sum_{k=-K}^{K+1} \alpha_k (u_{j+k} - u_{j+k-1}) = hu_y + O(h^{2K+3}) \tag{3.20}$$

and

$$\begin{aligned} z_{j+1/2} - z_{j-1/2} &= \sum_{l=-L}^{L+1} \beta_l (u_{j+l+1} - 2u_{j+1} + u_{j+l-1}) = h^2 (u_j)_{yy} + O(h^{2L+4}) \\ q_{j+1/2} - q_{j-1/2} &= \sum_{l=-L}^{L+1} \beta_l (u_{j+l+1} - 2u_{j+1} + u_{j+l-1}) = h^2 (u_j)_{yy} + O(h^{2L+4}) \end{aligned} \tag{3.21}$$

Hence, from the definition (3.9) of $P_{j+1/2}$, it is clear that

$$P_{j+1/2} - P_{j-1/2} = -h \left(\frac{\partial e}{\partial v} (v_j, w_j) \right)_y + O(h^{2K+3}) + h^2 \left(\frac{\partial e}{\partial v_y} (v_j, w_j) \right)_{yy} + O(h^{2L+4}),$$

that is,

$$P_{j+1/2} - P_{j-1/2} = hP(v_j, w_j) + O(h^{2K+3}) + O(h^{2L+4}) \tag{3.22}$$

holds.

Based on (3.20)–(3.22) we then find the equivalent equations of the scheme:

$$\begin{aligned} v_t - u_y &= O(h^{2K+2}), \\ u_t + P_y &= h(\mu(v)u_y)_y + O(h^{2K+2}) + O(h^{2L+3}), \\ w_t - z_y &= O(h^{2L+3}). \end{aligned}$$

It follows that the optimal choice is obtained for $K = L$, so that we find

$$\begin{aligned} v_t - u_y &= O(h^{2K+2}), \\ u_t + P_y &= h(\mu(v)u_y)_y + O(h^{2K+2}), \\ w_t - z_y &= O(h^{2K+3}). \end{aligned} \tag{3.23}$$

In Section 5 we will investigate several choice of parameters $K = L = 1, 2, 3$. For $K = L = 1$, we find

$$\begin{aligned} (\alpha_{-1}, \alpha_0, \alpha_1, \alpha_2) &= \left(\frac{-1}{12}, \frac{7}{12}, \frac{7}{12}, \frac{-1}{12} \right), \\ (\beta_{-1}, \beta_0, \beta_1) &= \left(\frac{-1}{12}, \frac{7}{6}, \frac{-1}{12} \right). \end{aligned}$$

For $K = L = 2$, we find

$$\begin{aligned} (\alpha_{-2}, \alpha_{-1}, \alpha_0, \alpha_1, \alpha_2, \alpha_3) &= \left(\frac{1}{60}, \frac{-2}{15}, \frac{37}{60}, \frac{37}{60}, \frac{-2}{15}, \frac{1}{60} \right), \\ (\beta_{-2}, \beta_{-1}, \beta_0, \beta_1, \beta_2) &= \left(\frac{1}{90}, \frac{-23}{180}, \frac{37}{30}, \frac{-23}{180}, \frac{1}{90} \right). \end{aligned}$$

For $K = L = 3$, we find

$$\begin{aligned} (\alpha_{-3}, \alpha_{-2}, \alpha_{-1}, \alpha_0, \alpha_1, \alpha_2, \alpha_3, \alpha_4) &= \left(\frac{-1}{280}, \frac{29}{840}, \frac{-139}{840}, \frac{533}{840}, \frac{533}{840}, \frac{-139}{840}, \frac{29}{840}, \frac{-1}{280} \right), \\ (\beta_{-3}, \beta_{-2}, \beta_{-1}, \beta_0, \beta_1, \beta_2, \beta_3) &= \left(\frac{-1}{560}, \frac{11}{504}, \frac{-779}{5040}, \frac{533}{420}, \frac{-779}{5040}, \frac{11}{504}, \frac{-1}{560} \right). \end{aligned}$$

Let us finally check the sign property (3.18) when the viscosity μ is constant. Consider the case $K = L = 1$. We have

$$\begin{aligned} \sum_{j=-\infty}^{+\infty} \sum_{k=-1}^1 \mu \beta_k m_{j+k} m_j &= - \sum_{j=-\infty}^{+\infty} \frac{\mu}{12} (-m_j m_{j-1} + 14m_j^2 - m_j m_{j+1}) \\ &= \frac{\mu}{6} \sum_{j=-\infty}^{+\infty} (7m_j^2 - m_j m_{j+1}). \end{aligned}$$

Since

$$(m_j - m_{j+1})^2 = m_j^2 + m_{j+1}^2 - 2m_j m_{j+1} \geq 0,$$

we have

$$\sum_{j=-\infty}^{+\infty} (m_j^2 - m_j m_{j+1}) \geq 0,$$

and

$$\frac{\mu}{6} \sum_{j=-\infty}^{+\infty} (7m_j^2 - m_j m_{j+1}) \geq 0.$$

This indeed implies the desired decreasing property (3.19). By a tedious but rather straightforward calculation, it can be checked that the same result holds in the other two cases $K = L = 2$ and $K = L = 3$.

4. SUBSONIC PHASE BOUNDARIES AND NONCLASSICAL SHOCKS

In this section we show that the schemes proposed in Section 3 allow us to compute subsonic (and supersonic) phase boundaries and nonclassical undercompressive shock waves. We are primarily interested in the van der Waals pressure law. However, it is convenient also to compare it with a cubic pressure law described below. Throughout, the time-discretization is based on a standard Runge–Kutta approach of sufficiently high order of accuracy. Except when specified otherwise, all the tests are done with the scheme in Section 2 corresponding to $K = L = 2$, so that the scheme is sixth order in space. All of the numerical solutions will be generated from an initial datum of the form

$$(v(x, 0), u(x, 0)) = \begin{cases} (v_l, u_l) & \text{for } x < 0, \\ (v_r, u_r) & \text{for } x > 0, \end{cases}$$

for some constant Riemann data to be specified. The viscosity and capillarity coefficients μ and λ will be taken to be constant.

4.1. Cubic Pressure Law

The van der Waals pressure can be well approximated by the cubic equation

$$p(v) = -(v - a)^3 + v + b, \quad v > 0, \quad (4.1)$$

where $a > 0$ and $b > 0$ are constants. In our experiments, for simplicity in the calculations, we take $a = 4$ and $b = 6$. See Fig. 1a for a representation of the graph of p . Setting

$$v_- = 4 - \frac{\sqrt{3}}{3}, \quad v_+ = 4 + \frac{\sqrt{3}}{3}, \quad (4.2)$$

three distinct regions can be distinguished:

(1) The interval $v \in [0, v_-]$ corresponds to the liquid phase: the system (2.19) is strictly hyperbolic and genuinely nonlinear.

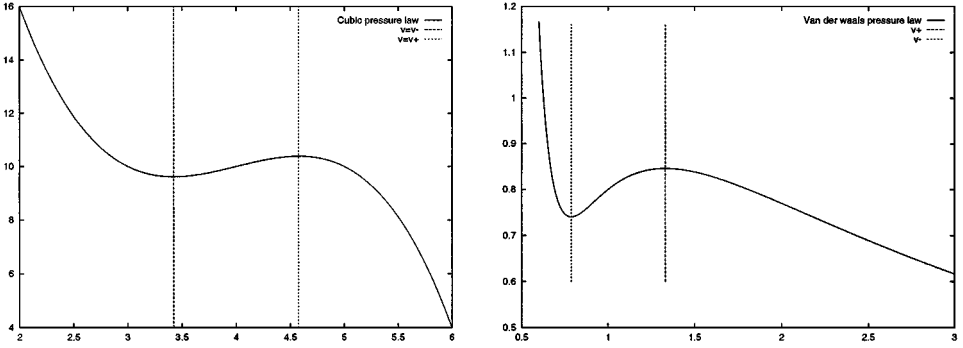


FIG. 1. (a) Cubic pressure law; (b) van der Waals pressure law.

- (2) In the interval $v \in [v_-, v_+]$, the system is of elliptic type.
- (3) The interval $v \in [v_+, \infty)$ corresponds to the vapor phase: the system (2.19) is strictly hyperbolic and genuinely nonlinear.

The so-called Maxwell stationary phase boundary, by definition corresponds to zero entropy dissipation. Here it connects $v = 3$ to $v = 5$ or vice versa.

Test 1: Propagating phase boundary. Figure 2 (v and u components) displays a typical subsonic phase boundaries, here propagating to the left, and preceded with a rarefaction wave. The dotted lines based on the critical values v_- and v_+ limit the hyperbolic and elliptic regions. The data for this test are

$$(\mu, \lambda) = (1, 0.2), \quad (v_l, u_l) = (3, 0), \quad (v_r, u_r) = (5, 2).$$

The mesh contains 600 points and the solution is represented at the time $t = 0.25$.

Test 2: Stationary phase boundary. Next, in Fig. 3 we used

$$(\mu, \lambda) = (1, 1.5), \quad (v_l, u_l) = (2.8, 0), \quad (v_r, u_r) = (5.2, 0).$$

The mesh contains 500 points and the solution is displayed at the time $t = 0.15$. We start here with a continuous velocity, which induces simply a stationary phase transition plus two rarefaction waves in each of the characteristic families. Not surprisingly the stationary

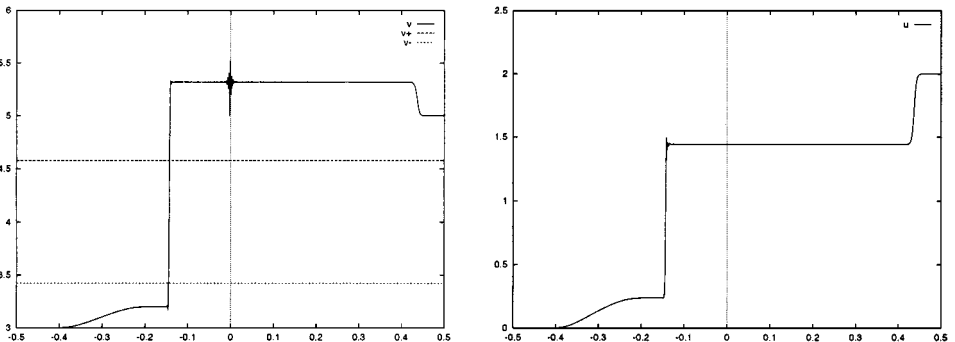


FIG. 2. Propagating phase boundary. (a) Volume component; (b) velocity component.

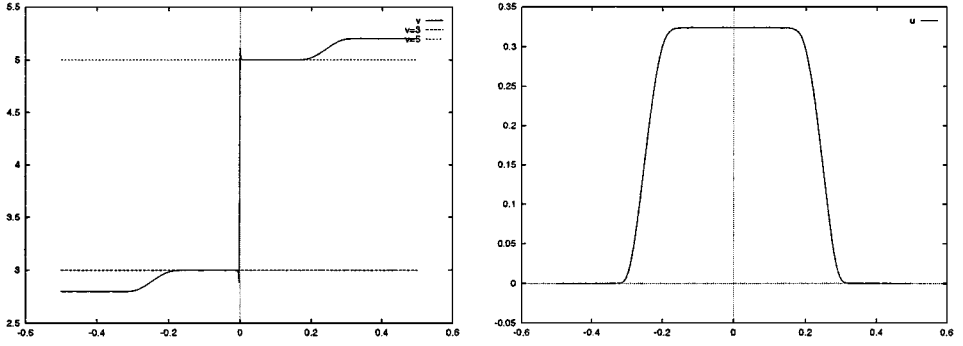


FIG. 3. Propagating phase boundary. (a) Volume component; (b) velocity component.

phase boundary satisfies the Maxwell condition; indeed it connects the values $v = 3$ to $v = 5$.

Test 3: Effect of the viscosity and capillarity coefficients. The solution depends on the relative values of the viscosity and capillarity coefficients. Indeed, in Fig. 4 using

$$\mu = 1, \quad (v_l, u_l) = (2.8, 0), \quad (v_r, u_r) = (5, 2),$$

and successively $\lambda = 0.1, 0.18, 0.25$, we obtain propagating phase boundaries propagating with various subsonic speeds. Here we used 800 mesh points and displayed the solution at the time $t = 0.22$.

Figure 5 illustrates that the phase boundaries are truly subsonic: the straight line connecting the two states cut the graph of the pressure.

4.2. Van der Waals Pressure Law

In the rest of this section we deal with the well-known van der Waals equation of state, given by

$$p(v, T) = \frac{RT}{v - b} - \frac{a}{v^2}, \quad (4.3)$$

where a, b, R are numerical constants and where the temperature $T > 0$ is fixed. We use

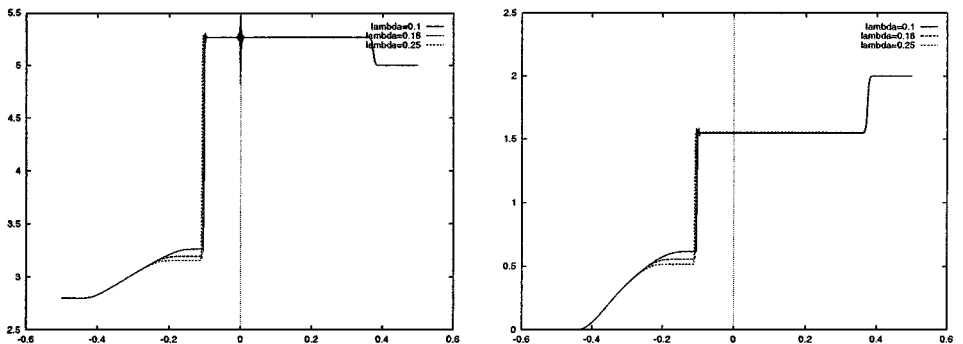


FIG. 4. Several values of λ . (a) Volume component; (b) velocity component.

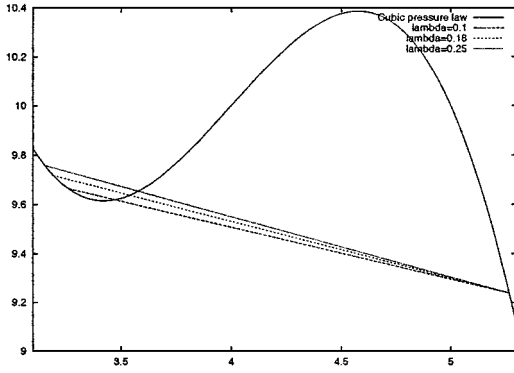


FIG. 5. Subsonic phase boundaries.

here the standard constants

$$a = 3, \quad b = \frac{1}{3}, \quad R = \frac{8}{3}, \tag{4.4}$$

and, for definiteness, the temperature is taken to be $T = 0.95$, just below the critical temperature $T = 1$. As in Section 4.1 on the cubic model, the system under consideration is hyperbolic and genuinely nonlinear in each on the regions $v < v_-$ and $v > v_+$, where, approximatively,

$$v_- = 0.787, \quad v_+ = 1.330.$$

The Maxwell line corresponds to the phase boundary connecting $v = 0.684$ (liquid) and $v = 1.727$ (vapor). Observe that the pressure is a convex function of v sufficiently small but a concave function for v sufficiently large.

Above the critical temperature, the model under consideration is always hyperbolic but is not always genuinely nonlinear; see Section 4.3.

Test 4: Propagating phase boundary. Figure 6 displays a propagating phase transition obtained from the following data:

$$(\mu, \lambda) = (0.1, 1e - 5), \quad (v_l, u_l) = (0.6, -2), \quad (v_r, u_r) = (1.5, 0).$$

We used a mesh with 1000 points and we represent the solution at the time $t = 0.15$.

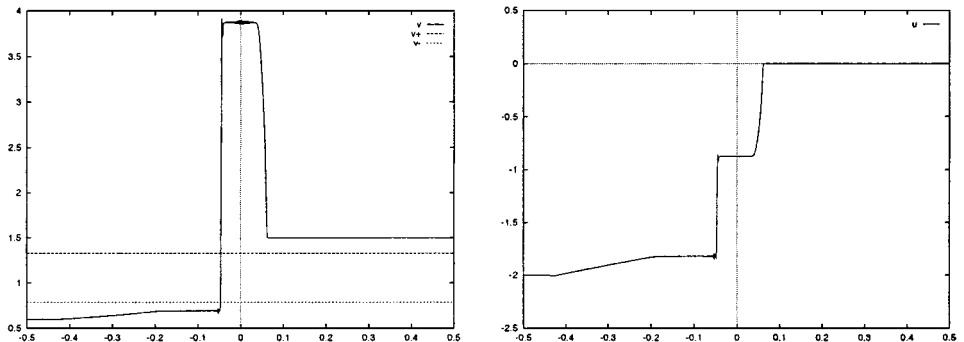


FIG. 6. Propagating phase boundary. (a) Volume component; (b) velocity component.

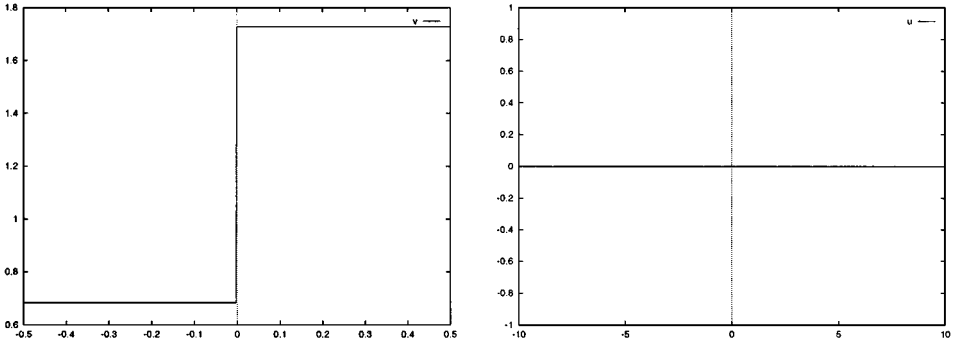


FIG. 7. Stationary phase boundary. (a) Volume component; (b) velocity component.

Test 5: Stationary phase boundary. In Fig. 7, the test was performed with

$$(\mu, \lambda) = (0.1, 1e-3), \quad (v_l, u_l) = (0.684117091, 0), \quad (v_r, u_r) = (1.72700257, 0).$$

The initial jump is very close to the Maxwell stationary phase boundary and, as expected, the scheme keeps the Maxwell discontinuity stationary. The mesh contains 600 points and the solution is displayed at the time $t = 0.20$.

Test 6: Effect of the viscosity and capillarity coefficients. Finally, as in Test 3, we demonstrate that the solutions depend on the relative sizes of the viscosity and capillarity parameters. Let us use

$$\mu = 0.1, \quad (v_l, u_l) = (0.675, -1.45), \quad (v_r, u_r) = (0.75, 0),$$

together with several values of capillarity $\lambda = 10^{-5}, 0.1, 0.75$. See Fig. 8. The solution contains two (symmetric) propagating phase boundaries with opposite speeds. The mesh contains 800 points and the solution is represented at the time $t = 0.22$.

Figure 9 illustrates that the phase boundaries are truly subsonic: the straight line connecting the two states cut the graph of the pressure.

4.3. Nonclassical Shock Waves in the Hyperbolic Regime

Above the critical temperature (that is, $T > 1$ in normalized units), the van der Waals model is strictly hyperbolic, even though it is not always genuinely nonlinear. In this

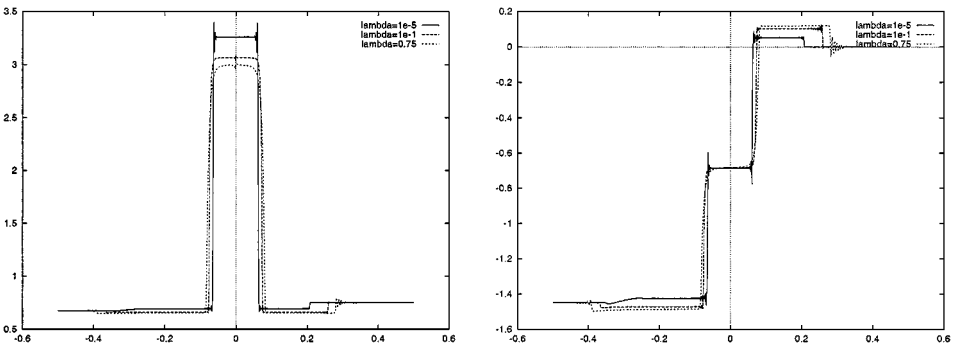


FIG. 8. Several values of λ . (a) Volume component; (b) velocity component.

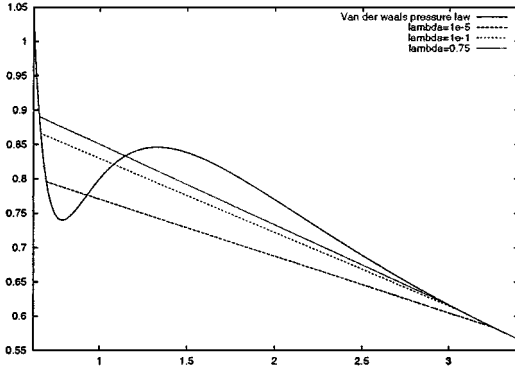


FIG. 9. Subsonic phase boundaries.

hyperbolic regime, instead of subsonic phase boundaries, the equations may exhibit non-classical shock waves. This is illustrated below. Recall that the cubic equation of state in the hyperbolic regime was dealt with by Hayes and LeFloch in [15].

We choose now $T = 1.005$. Figure 10 represents the graph of the corresponding pressure law.

The viscosity coefficient is fixed to be 0.1. The mesh size is 1000 points and $K = L = 2$ as before. Figure 11 shows a nonclassical shock obtained with the following values:

$$(v_l, u_l) = (0.8, 0), \quad (v_r, u_r) = (1.5, 1), \quad \lambda = 0.001.$$

Figure 12 shows the dependence of this solution with respect to the capillarity coefficient.

Figure 13 illustrates that shocks are truly nonclassical: the straight line connecting the two states cuts the graph of the pressure.

5. KINETIC FUNCTIONS

To characterize the dynamics of subsonic phase boundaries and nonclassical shock waves, we now determine numerically the kinetic functions associated with the schemes introduced in Section 3. Precisely, we compute the right-hand value of the volume as a function of

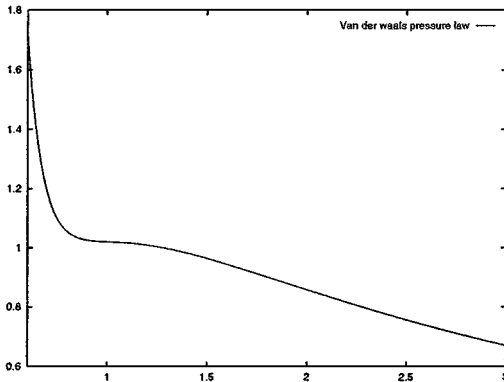


FIG. 10. Van der Waals pressure law ($T = 1.005$).

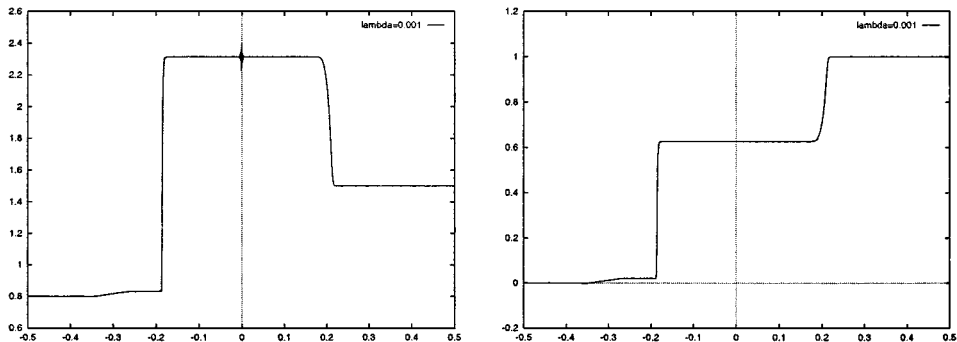


FIG. 11. Nonclassical shock wave (Van der Waals). (a) Volume; (b) speed.

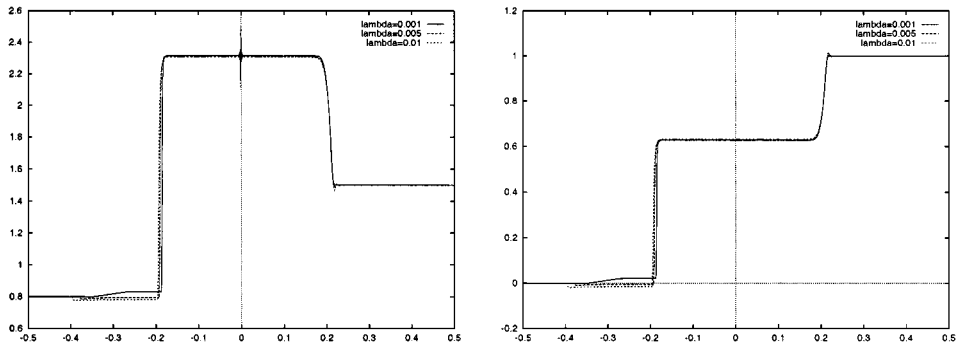


FIG. 12. Several values of λ . (van der Waals law). (a) Volume; (b) speed.

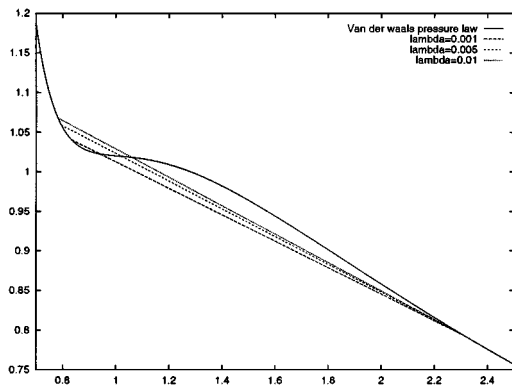


FIG. 13. Nonclassical shock on the pressure plot.

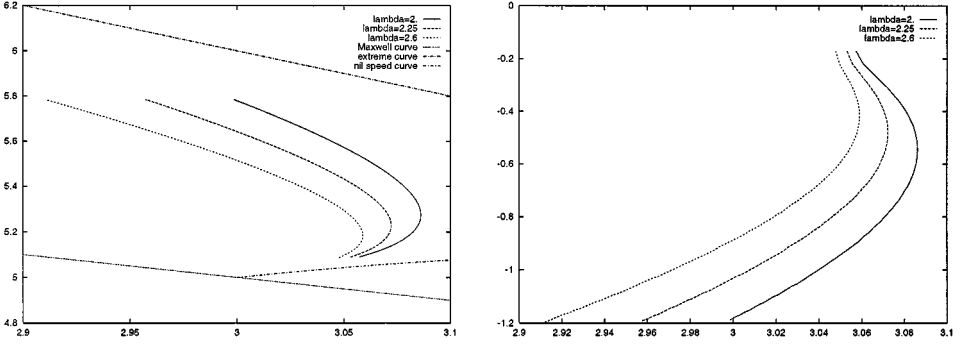


FIG. 14. Several values of λ (cubic law). (a) Volume; (b) speed.

the left-hand state. We also compute the propagation speed of the phase boundaries or the nonclassical shocks. As will become clear from the plots below, the kinetic functions depend on the viscosity/capillarity ratio (more precisely on μ^2/λ) and on the specific scheme under consideration as well.

Together with the kinetic functions, we plot also some extremal curves which are known to limit the range of the kinetic functions, especially the curve along which the entropy dissipation vanishes and the (Maxwell) curve along which the shock speed vanishes.

Kinetic functions for several capillarity coefficients. Figure 14 concerns the cubic pressure law (4.1). In all of the runs we used the following initial data:

$$(v_l, u_l) = (3, 0), \quad v_r = 5.$$

The viscosity is taken to be $\mu = 2$ and the mesh contains 1200 points. We computed three distinct kinetic curves associated with different values of the capillarity coefficient. A point on the curve is associated with a propagating phase boundary found for some given initial velocity u_r . Each curve is obtained by letting u_r describe the interval $[0.6, 5]$.

Figure 15 concerns the van der Waals pressure law (4.3). We choose here the initial data

$$(v_l, u_l) = (0.666, -1.8), \quad v_r = 0.75.$$

The viscosity is $\mu = 0.1$ and the mesh contains 1200 points. Here each curve is obtained for u_r describing the interval $[-1.8, 0]$.

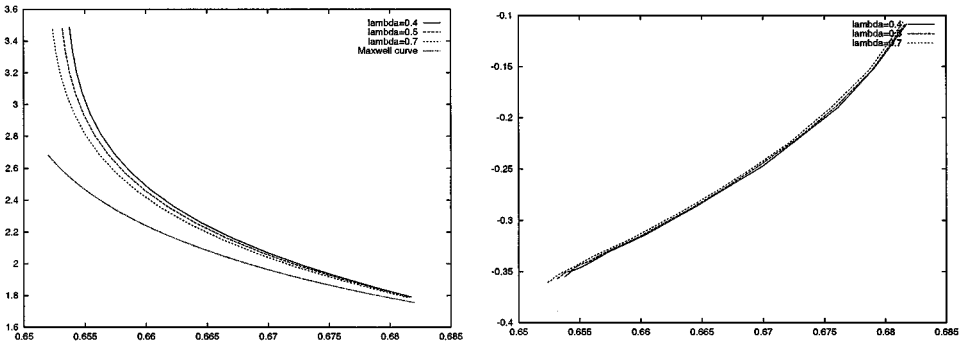


FIG. 15. Several values of λ (van der Waals). (a) Volume; (b) speed.

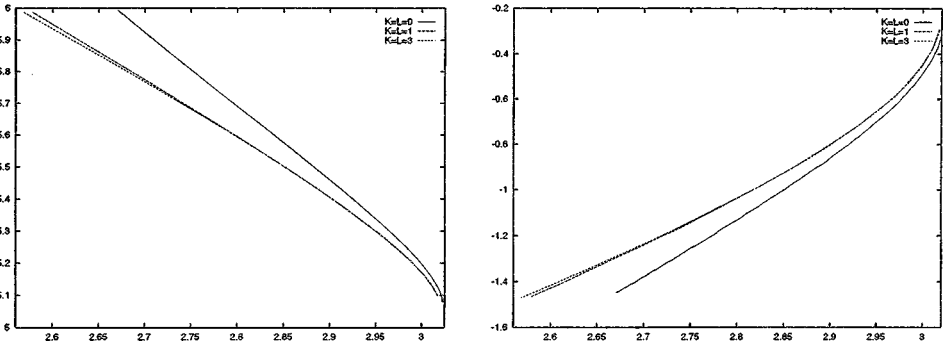


FIG. 16. Several values of K and L (cubic law). (a) Volume; (b) speed.

Kinetic functions for several schemes. Next we study the effect of the order of accuracy of the scheme on the kinetic curves (Cubic law). For definiteness we fix the following constants:

$$(v_l, u_l) = (3, 0), \quad v_r = 5, \quad \lambda = 1.5, \quad \beta = 1.$$

Similarly as above, we compute kinetic curves by letting v_l describe the interval $[0.6, 10]$. Figure 16 displays the results for several choices of the parameters K and L .

6. CONCLUSIONS

In this paper, we dealt with propagating phase boundaries modeled by the isothermal model of compressible fluids governed by van der Waals-type equations of state.

Capillarity effects were taken into account by using the derivative of the specific volume, v_y , as an independent variable. We have introduced a new class of entropy conservative numerical schemes in the sense of Tadmor. These schemes are endowed with nonlinear stability properties: the total energy—which plays the role of a mathematical entropy in the sense of Lax—is decreasing in time, the decay being due to the viscosity only. Hence, we were able to reproduce at the discrete level an important property satisfied by the physical model. We also established that the proposed schemes may have sufficiently high order of accuracy, so that the corresponding equivalent equation coincide with the continuous model up to $O(h^3)$ at least.

We demonstrated the existence of propagating subsonic phase boundaries and of nonclassical undercompressive shock waves for the van der Waals model. The proposed schemes successfully computed these undercompressive waves. Nonsteady subsonic boundaries (not consistent with the standard Maxwell construction) are not found in thermodynamics textbooks nor in the Riemann solvers derived in [23] and [12]. Subsonic phase boundaries are induced precisely by the capillarity effects, kept in balance with the viscosity effects. The former create oscillations while the latter introduce dissipation in the equations. The small-scale effects are dominant in determining the dynamics of undercompressive waves. The observed oscillations are entirely expected and standard numerical methods such as the TVD schemes are clearly not adapted.

Following [15], kinetic relations associated with the schemes were numerically determined. These curves depend on the order of the schemes and also on the relative strength

of the viscosity and capillarity coefficients. The kinetic curves allow us to compare the properties of the schemes.

The equivalent equation provides only some indication of the behavior of the schemes. For sufficiently small propagation speed good agreement has been observed. But, for waves with sufficiently large speed or large amplitude, some discrepancy does arise. This is a central difficulty with dissipation-sensitive problems.

We have encountered some specific numerical difficulties with the van der Waals pressure law, due to its shape. In normalized units at least and in the range of interest near the inflection point, the subsonic phase boundaries connect states having very different characteristic speeds. Indeed, the sound speed in the liquid tends to infinity as the volume v tends to zero, while for large v in the vapor phase the sound speeds tends to zero. This appears clearly in Fig. 1b. (This behavior is not found for the cubic law in Fig. 1a.) This has dramatic consequences from the numerical standpoint. A small error in the liquid state corresponds to a large error in the vapor one. As a consequence, finding numerically the range of left- and right-hand states for which subsonic phase boundaries exist has been particularly challenging. Then, nonclassical shock waves and subsonic phase boundaries may also be particularly delicate to observe in practical situations.

Finally, we point out that extending the present approach to the viscosity–capillarity model of van der Waals fluids based on three conservation laws (mass, momentum, and energy) should be possible. Many of the properties derived here generalize immediately to this model.

REFERENCES

1. R. Abeyaratne and J. K. Knowles, Kinetic relations and the propagation of phase boundaries in solids, *Arch. Rational Mech. Anal.* **114**, 119 (1991).
2. R. Abeyaratne and J. K. Knowles, Implications of viscosity and strain gradient effects for the kinetics of propagating phase boundaries, *SIAM J. Appl. Math.* **51**, 1205 (1991).
3. M. Affouf and R. Caflisch, A numerical study of Riemann problem solutions and stability for a system of viscous conservation laws of mixed type, *SIAM J. Appl. Math.* **51**, 605 (1991).
4. C. Chalons and P. G. LeFloch, A fully discrete scheme for diffusive-dispersive conservation laws, *Numerische Math.* (2001), to appear.
5. B. Cockburn and H. Gau, A model numerical scheme for the propagation of phase transitions in solids, *SIAM J. Sci. Comput.* **17**, 1092 (1996).
6. H. T. Fan, A limiting “viscosity” approach to the Riemann problem for materials exhibiting a change of phase II, *Arch. Rational Mech. Anal.* **116**, 317 (1992).
7. H. T. Fan, The uniqueness and stability of the solution of the Riemann problem of a system of conservation laws of mixed type, *Trans. Am. Math. Soc.* **333**, 913 (1992).
8. H. T. Fan, A vanishing viscosity approach on the dynamics of phase transitions in van der Waals fluids, *J. Differential Equations* **103**, 179 (1993).
9. H. T. Fan, One-phase Riemann problem and wave interactions in systems of conservation laws of mixed type, *SIAM J. Math. Anal.* **24**, 840 (1993).
10. H. T. Fan and M. Slemrod, The Riemann problem for systems of conservation laws of mixed type, in *Shock Induces Transitions and Phase Structures in general media*, edited by R. Fosdick, E. Dunn, and H. Slemrod, IMA Vol. Math. Appl. 52 (Springer-Verlag, New York, 1993), p. 61.
11. S. Gavrilyuk and H. Gouin, A new form of governing equations of fluids arising from Hamilton’s principle, *Int. J. Eng. Sci.* **37**, 1495 (1999).

12. H. Hattori, The Riemann problem for a van der Waals fluid with the entropy rate admissibility criterion, *Arch. Rational Mech. Anal.* **92**, 247 (1986).
13. B. T. Hayes and P. G. LeFloch, Nonclassical shocks and kinetic relations: Scalar conservation laws, *Arch. Rational Mech. Anal.* **139**, 1 (1997).
14. B. T. Hayes and P. G. LeFloch, Nonclassical shocks and kinetic relations: Finite difference schemes, *SIAM J. Numer. Anal.* **35**, 2169 (1998).
15. B. T. Hayes and P. G. LeFloch, Nonclassical shocks and kinetic relations: Strictly hyperbolic systems, *SIAM J. Math. Anal.* **31**, 941 (2000).
16. D. Jacobs W. R. McKinney, and M. Shearer, Traveling wave solutions of the modified Korteweg-deVries Burgers equation, *J. Differential Equations* **116**, 448 (1995).
17. R. D. James, The propagation of phase boundaries in elastic bars, *Arch. Rational Mech. Anal.* **73**, 125 (1980).
18. S. Jin, Numerical integrations of systems of conservation laws of mixed type, *SIAM J. Appl. Math.* **55**, 1536 (1995).
19. P. G. LeFloch, Propagating phase boundaries: Formulation of the problem and existence via the Glimm scheme, *Arch. Rational Mech. Anal.* **123**, 153 (1993).
20. P. G. LeFloch, An introduction to nonclassical shocks of systems of conservation laws, in *Proceedings of the International School on Theory and Numerics for Conservation Laws, Freiburg Littenweiler (Germany), 20–24 October 1997*, edited by D. Kröner, M. Ohlberger, and C. Rohde, Lecture Notes in Computational Science and Engineering, (1998), p. 28.
21. P. G. LeFloch, *Hyperbolic Systems of Conservation Laws: The Theory of Classical and Nonclassical Shock Waves*, E.T.H. Lecture Notes Series, 2001, to appear.
22. P. G. LeFloch and C. Rohde, High-order schemes, entropy inequalities, and nonclassical shocks, *SIAM J. Numer. Anal.* **37**, 2023 (2000).
23. M. Shearer, The Riemann problem for a class of conservation laws of mixed type, *J. Differential Equations* **46**, 426 (1982).
24. M. Shearer and Y. Yang, The Riemann problem for the p-system of conservation laws of mixed type with a cubic nonlinearity, *Proc. Roy. Soc. Edinburgh.* **125A**, 675 (1995).
25. C.-W. Shu, A numerical method for systems of conservation laws of mixed type admitting hyperbolic flux splitting, *J. Comput. Phys.* **100**, 424 (1992).
26. M. Slemrod, Admissibility criteria for propagating phase boundaries in a van der Waals fluid, *Arch. Rational Mech. Anal.* **81**, 301 (1983).
27. M. Slemrod, Lax-Friedrichs and the viscosity–capillarity criterion, in *Physical Mathematics and Nonlinear Partial Differential Equations*, edited by S. M. Rankin and J. H. Lightbourne (Marcel Dekker, New York, 1985), p. 75.
28. M. Slemrod, A limiting “viscosity” approach to the Riemann problem for materials exhibiting a change of phase I, *Arch. Rational Mech. Anal.* **105**, 327 (1989).
29. M. Slemrod and J. E. Flaherty, Numerical integration of a Riemann problem for a van der Waals fluid, in *Phase Transformations*, edited by C. A. Elias and G. John (Elsevier, Amsterdam, 1986).
30. E. Tadmor, Entropy conservative finite element schemes, in *Numerical methods for Compressible Flows Finite Difference Element and Volume Techniques*, Proc. Winter Annual Meeting, Amer. Soc. Mech. Eng, AMD-Vol. 78, edited by T. E. Tezduyar and T. J. R. Hughes (1986), p. 149.
31. E. Tadmor, The numerical viscosity of entropy stable schemes for systems of conservation laws, *Math. Comput.* **49**, 91 (1987).
32. L. Truskinovsky, Dynamics of non-equilibrium phase boundaries in a heat conducting nonlinear elastic medium, *J. Appl. Math. Mech.* **51**, 777 (1987).
33. L. Truskinovsky, Kinks versus shocks, in *Shock Induced Transitions and Phase Structures in General Media*, edited by R. Fosdick, E. Dunn, and H. Slemrod, IMA Vol. Math. Appl. 52 (Springer-Verlag, New York 1993).